A system for controlling the directivity of sound radiated from a structure

Nikolaos Kournoutos[1] and Jordan Cheer[1, a)]

Institute of Sound and Vibration Research, University of Southampton, Southampton, SO17 1BJ, United Kingdom

(Dated: 13 December 2019)

Directional sound fields can be generated by arrays of multiple sound sources such as loudspeaker drivers. These systems, though potentially capable of high levels of directivity control over a broad bandwidth, may prove prohibitively expensive, fragile, or impracticable in certain applications. To overcome these limitations, this paper presents an investigation into the design and limitations of a directional structural-actuator-based array. This provides an affordable and robust alternative to conventional loudspeakers, particularly when the actuators can be used to radiate via a pre-existing structure and where the required audio quality is lower, or the bandwidth somewhat limited. In the first instance, an analytical model is formulated, and used to perform a simulation-based parametric study, which provides insights into the design trade-offs. Based on this study, a physical prototype is constructed using six actuators and a flat panel, which enables the model to be experimentally validated and an evaluation of the directional radiation capabilities of the proposed system to be carried out. Experiments show that the simple analytical model is an effective tool in designing such arrays, predicting the trends in the behaviour of the prototype, and that the structural actuator-based system is capable of controlling directivity within its intended operational bandwidth.

[a)]j.cheer@soton.ac.uk

I. INTRODUCTION

The most straightforward way of achieving control over the directional characteristics of a radiated sound field has been through the use of multiple individual acoustic sources. The majority of relevant research has thus focused on developing methods for directivity control using arrays of conventional, fixed directivity loudspeakers as sources[1–4], or even variable directivity drivers[5] and parametric arrays[6]. Such systems have been shown to be effective and have been investigated for various applications ranging from personal entertainment[7,8] to automotive safety[9,10]. Despite their performance, however, the cost of installing such arrays may potentially prove too high, and necessitate undesired, or impractical modifications to the host system, such as the opening of holes in a structure to act as the loudspeaker grille and allow the loudspeakers to radiate. Moreover, this may also limit the robustness of these loudspeaker-based systems in harsh operating environments, where the loudspeakers would be directly exposed to water and dirt.

Instead of using loudspeaker drivers, which may be too heavy, costly or fragile for the intended implementation, a sound radiating system can be designed around the vibration of a panel by introducing a controlled distribution of forces. Dynamic force actuators attached to a panel can excite its structural response, which in turn will generate acoustic radiation and such an arrangement has already been used as an alternative to conventional loudspeakers. Such Distributed Mode Loudspeakers (DMLs) have been shown to be capable of omnidirectional acoustic radiation over a greater bandwidth when compared to conventional loudspeakers using a cone to achieve acoustic radiation[11,12], but with a reduced low

frequency response[13]. It has also been shown that this performance can be improved by using multiple optimally driven actuators on the panels[14].

A directional system based on such a structurally driven radiating surface could prove useful in applications where exposure of a loudspeaker to specific environmental conditions could prove damaging to the system, or interventions to the structure in order to install a conventional loudspeaker array would be cost inefficient. Such applications potentially include public displays, from advertising boards to museum and gallery displays, personal entertainment systems utilizing DMLs or even flat screen TV monitors, as well as warning sound systems integrated into hybrid and electric vehicles[16]. In addition, using a vibrating panel to radiate a directional sound field could increase the limit that occurs due to the aliasing, which is associated with the discrete nature of a loudspeaker array and imposes a high frequency limit on the system[15]. By interpolating sound pressure between the locations of the actuators, a vibrating panel may potentially reduce these aliasing effects, although the radiated sound field is also likely to be affected by its modal vibration behaviour.

Methods of controlling the sound radiation from a vibrating panel excited by an external disturbance have included passive modifications, such as the attachment of ribs and supports to the structure[17], as well as the application of force through active elements such as piezo-ceramic[18] or inertial actuators[19]. Control of the radiated sound field through manipulating the vibration of such panels has been the focus of significant research in active control[20,21], with the majority of this work having focused on reducing the sound radiated by structural vibration[22,23]. Although the directional aspects of the radiated sound fields produced

by structural vibration have been investigated[24], relatively little research has focused on controlling these vibrations to produce sound fields with specific directional characteristics.

In this paper, a directional sound system is developed utilizing an array of inertial actuators attached to a flat panel. A simple analytical model is used in order to simulate the system and enable an investigation into the effects that different parameters have on its performance. Upon consideration of the simulation results, a prototype system is constructed and tested in an anechoic chamber. These experimental results are analysed to determine the directivity performance of the developed system and they are also compared to the simulation results to evaluate the accuracy of the mathematical model and, therefore, the presented parametric study.

Section II will lay out the principle of operation of the system, and present the analytical mathematical model used to simulate the system. A method to control the directivity of the system and a metric for its quantitative evaluation will be presented in Sec. III, and in Sec. IV results from the simulation-based parametric study of the system will be presented and discussed. Section V will be devoted to describing the experimental evaluation of a prototype implementation in an anechoic environment, and a comparison between the results from the physical system and the simulations. Finally, Sec. VI will summarize and conclude this paper.

II. MODEL OF SOUND RADIATION FROM A FLAT PANEL DRIVEN BY MULTIPLE ACTUATORS

Vibrating structures generate acoustic radiation by imposing fluctuations on the pressure field. These fluctuations depend on both the response of the structure and on how the structure is excited. For example, a plate radiates differently depending on its construction, but also on the excitation force. Therefore, by controlling the vibration of a structure, it is possible to control how it radiates and this can be achieved using multiple inertial actuators mounted to the structure. In this section, an analytical model will be presented to enable the exploration in the following sections of the concept of controlling the directivity of sound radiation from a flat panel using an array of structural actuators.

The proposed system can be approximated by a thin rectangular panel, simply supported along all four of its edges, with a distribution of points along its surface at which a transverse force, f_i, is applied. Figure 1 shows a schematic of this simplified system with six point forces distributed along the length of a panel with dimensions $a \times b \times h$. The model that will be used to estimate the pressure at locations in the far field due to the vibrating panel can be divided into two principal parts: the vibration of the panel by a force distribution, and the far field sound radiation of sound that results from this vibration.

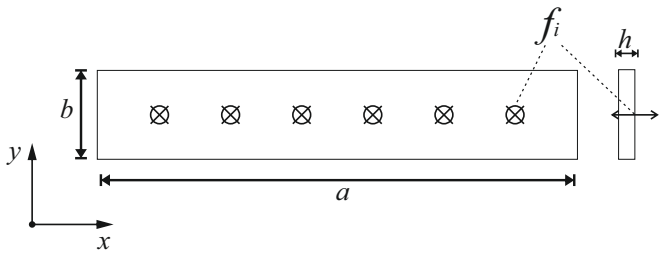

FIG. 1. Schematic of the modeled system, consisting of a rectangular panel of dimensions $a \times b \times h$ excited by a distribution of individual transverse point forces, f_i.

A. Structural response of a thin rectangular panel

The motion of a thin rectangular panel can be expressed in terms of its transverse displacement, w, as[25]

$$EI_M \left(\frac{\partial^4 w}{\partial x^4} + 2\frac{\partial^4 w}{\partial x^2 \partial y^2} + \frac{\partial^4 w}{\partial y^4} \right) + \rho h \frac{\partial^2 w}{\partial t^2} = -f(x, y, t), \tag{1}$$

where E is Young's modulus, I_M is the moment of inertia, ρ is the density, x and y are the coordinate directions, t is the time, and $f(x, y, t)$ corresponds to the applied forcing function, which is zero in the case of free motion. The quantity EI_M is equivalent to the bending stiffness of the panel, and it is convenient to express this using the Poisson ratio of the panel material, ν, which gives

$$EI_M = \frac{h^3 E}{12(1-\nu^2)}. \tag{2}$$

It is important to stress that for Eq.(1), the wavelength of vibration is assumed to be much greater than the thickness of the panel and no transverse shear or rotary inertia are taken into account. These approximations limit the accuracy of this mathematical model to low frequencies[25], which will be discussed further in Section V.

A continuous system, such as the one formulated above and described by Eq. (1), can be approximated as a multiple degree of freedom system, as shown by Meirovitch[26]. A separable solution of the transverse modal displacement can be chosen for the free motion of a simply supported panel as

$$w_{mn}(x,y,t) = W_{mn}\sin(k_m x)\sin(k_n y)\mathrm{e}^{\mathrm{j}\omega t}, \tag{3}$$

where m and n are the modal indices for modes along the x and y axes respectively, and W_{mn} is the corresponding modal amplitude. The mode shapes of a panel have been thoroughly studied, and are dependent on its boundary conditions[27]. For simply supported boundaries of zero transverse displacement along the edges, the wavenumbers in each coordinate direction are

$$k_m = m\pi/a, \quad m = 1,2,3,... \tag{4a}$$

$$k_n = n\pi/b, \quad n = 1,2,3,... \tag{4b}$$

and the discrete frequencies at which the system resonates are given by

$$\omega_{mn} = \left(\frac{EI}{\rho h}\right)^{1/2}\left[k_m^2 + k_n^2\right]. \tag{5}$$

In order to represent the effects of an inertial actuator acting upon the panel, it is necessary to describe the response of the system to a harmonic force. This means that the right-hand side term in Eq. (1) becomes a two-dimensional forcing function $f(x,y)e^{\mathrm{j}\omega t}$. The forced response can then be written as a summation over the modes of the free response of the panel, vibrating at the forcing frequency, such that

$$w_{mn}(x,y,t) = \sum_{m=1}^{\infty}\sum_{n=1}^{\infty} W_{mn}\sin(k_m x)\sin(k_n y)\mathrm{e}^{\mathrm{j}\omega t}. \tag{6}$$

The most straightforward type of input is a point force input, expressed as $f_i(x, y, t) = F_i\delta(x - x_i)\delta(y - y_i)e^{j\omega t}$ and located at x_i, y_i. Under such conditions, the modal amplitudes are given by

$$W_{mn}(i) = \frac{4F_i \sin k_m x_i \sin k_n y_i}{M(\omega^2 - \omega_{mn}^2)}, \tag{7}$$

where $M = \rho hab$ is the total mass of the panel. For a distribution of I point forces acting upon the panel, the expression for the sum of the modal amplitudes has the form

$$\sum_{i=1}^{I} W_{mn}(i) = \frac{4}{M(\omega^2 - \omega_{mn}^2)} \sum_{i=1}^{I} F_i \sin k_m x_i \sin k_n y_i. \tag{8}$$

The solution stemming from Eqs. (6) and (8) is generally well suited to determine the global system response. However, it is not well suited to predict structural near-field effects at higher frequencies. To ensure accuracy at higher frequencies, a relatively high number of modes is necessary to approximate the sum in Eq. (6) when it is truncated in the calculation of the structural response[28].

The effect of each inertial actuator on the thin panel can be approximated by a single point force acting at its respective location. However, as practical actuators have a finite area of contact with the panel, such an approximation may lead to inaccuracies at higher frequencies, where the corresponding wavelengths are comparable to the dimensions of the actuator. This potential inaccuracy can be reduced by representing each actuator using a number of point forces, distributed over its contact area, acting in phase and with the same amplitude. Figure 2 shows the distribution of point forces, eight per actuator, that will be used in the subsequent simulations. Another factor that has not been included in the model is the mass of the actuators, which may have an effect on the response of the panel due to

mass loading. A more detailed model, which represents the actuators as mass-spring-damper systems has been explored in[29], however, the effect of the added mass on the panel will not be considered further in the present model.

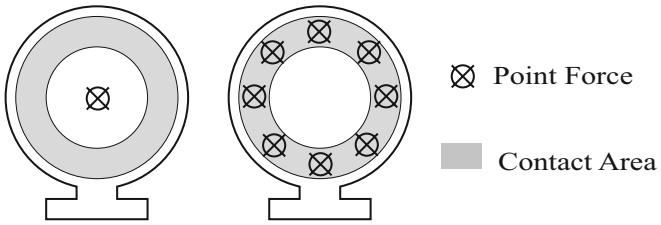

FIG. 2. Approximation of an example actuator using either a single point force or a distribution of point forces acting over its contact area.

B. Sound radiation from the panel to the acoustic far field

The acoustic pressure in the far field, at a distance r from the defined centre point of the panel, can be calculated using the Rayleigh integral in terms of the complex transverse velocities $\dot{w}(\boldsymbol{r}_S)$ at points $\boldsymbol{r}_S$ on the surface S, such that the pressure is given by

$$p\left(\boldsymbol{r}\right) = \int_S \frac{\mathrm{j}\omega\rho_0\dot{w}(\boldsymbol{r}_s)\mathrm{e}^{-\mathrm{j}kR}}{2\pi R}\mathrm{d}S, \tag{9}$$

where $R = |\boldsymbol{r} - \boldsymbol{r}_s|$, and the frequency dependence has been dropped for notational convenience. This formulation assumes that the panel is mounted on an infinite baffle. The complex velocity $\dot{w}(\boldsymbol{r}_S)$ derived from Eqs. (6) and (8) is

$$\dot{w}(\boldsymbol{r}_S) = \dot{W}_{mn}\sin\left(\frac{m\pi x}{a}\right)\sin\left(\frac{n\pi y}{b}\right) \qquad \{^{0\leq x\leq a}_{0\leq y\leq b}\}. \tag{10}$$

The total acoustic pressure radiated from the panel due to vibration at its (m,n)-th mode at a point described by the coordinates (r,θ,ϕ) in the far field, is expressed upon evaluation

of the integral in Eq. (9) using the transverse modal displacement of Eq. (6) as

$$p_{m,n}(r,\theta,\phi) = \frac{\mathrm{j}\omega\rho_0\dot{W}_{mn}\mathrm{e}^{-\mathrm{j}kr}}{2\pi r}\ldots \\ \ldots\int_0^b\int_0^a \sin\left(\frac{m\pi x}{a}\right)\sin\left(\frac{n\pi y}{b}\right)\mathrm{e}^{\mathrm{j}(\alpha x/a+\beta y/b)}\mathrm{d}x\,\mathrm{d}y, \quad (11)$$

where $\alpha = ka\sin\theta\cos\phi$ and $\beta = kb\sin\theta\sin\phi$. The above integral can be evaluated as in[30], which yields the pressure due to the (m,n)-th mode as

$$p_{m,n}(r,\theta,\phi) = \frac{\mathrm{j}\omega\rho_0\dot{W}_{mn}\mathrm{e}^{-\mathrm{j}kr}}{2\pi r}\frac{ab}{mn\pi^2}\ldots \\ \ldots\left[\frac{(-1)^m\mathrm{e}^{-\mathrm{j}\alpha}-1}{(\alpha/m\pi)^2-1}\right]\left[\frac{(-1)^n\mathrm{e}^{-\mathrm{j}\beta}-1}{(\beta/n\pi)^2-1}\right]. \quad (12)$$

Taking into consideration a number of I point forces acting at coordinates (x_i, y_i), and M and N modes along the x and y directions, respectively, the above equation can be used in conjunction with Eq. (8) to calculate the pressure radiated from the panel due to the actuator array, provided a sufficient number of modes is used. This pressure is expressed as a triple summation of the form

$$p(r,\theta,\phi) = \sum_{i=1}^{I}\sum_{m=1}^{M}\sum_{n=1}^{N}\frac{\mathrm{j}\omega\rho_0\mathrm{e}^{-\mathrm{j}kr}}{2\pi r}\frac{ab}{mn\pi^2}\ldots \\ \ldots\left[\frac{(-1)^m\mathrm{e}^{-\mathrm{j}\alpha}-1}{(\alpha/m\pi)^2-1}\right]\left[\frac{(-1)^n\mathrm{e}^{-\mathrm{j}\beta}-1}{(\beta/n\pi)^2-1}\right]\dot{W}_{mn}(i). \quad (13)$$

It is important to finally note that the mathematical model presented in this section assumes an infinite baffle upon which the vibrating panel is set. As this configuration would not be straightforward to replicate in the experimental validation process, or present a practical realization of the proposed array system, the simulations and measurements will only consider radiation in the forward half-space.

III. DIRECTIVITY CONTROL STRATEGY

In loudspeaker arrays, acoustic beamforming is achieved through the control of the relative amplitudes and phases of the individual loudspeakers. In the system proposed in this paper, the vibration of the panel determines the radiated sound field and this is controlled by adjusting the relative amplitudes and phases of the inertial actuators. There are a variety of methods of optimizing the relative amplitudes and phases of the individual elements in an array to achieve a directional response, however, when the primary objective is to maximize the difference in sound pressure level between different regions of space, the acoustic contrast maximization process has been shown to offer the highest level of performance[31,32]. Therefore, this method has been adopted here and will be described for the present application in Section III A.

A. Acoustic contrast maximization

The acoustic contrast maximization method was proposed by Choi and Kim[33] and aims to maximize the acoustic contrast between the mean square pressure in two distinct zones defined as bright and dark, respectively referring to the regions where sound needs to be generated or attenuated. Figure 3 illustrates an example with a 36° wide bright zone and a supplementary dark zone covering the remaining half-space in front of a six source array.

For an array of I sources driven by a vector of complex input signals, $\boldsymbol{u}$, at a given frequency, the complex pressure amplitudes calculated by Eq. (13), $\boldsymbol{p}$, are given by vectors $\boldsymbol{p}_B$ and $\boldsymbol{p}_D$ for M_B measurement points in the bright and M_D points in the dark zone respec-

tively. The complex transfer responses between the sources and the pressure measurement points in the bright and dark zones are $\boldsymbol{G}_B$ and $\boldsymbol{G}_D$, so that

$$\boldsymbol{p}_B = \boldsymbol{G}_B \boldsymbol{u} \qquad \boldsymbol{p}_B = \boldsymbol{G}_D \boldsymbol{u}. \tag{14}$$

Taking the above into account, the acoustic contrast is defined at a given frequency as the ratio of the mean of the squared pressures in the bright zone and the dark zone, which can be expressed as

$$C = \frac{M_D \boldsymbol{p}_B^H \boldsymbol{p}_B}{M_B \boldsymbol{p}_D^H \boldsymbol{p}_D} = \frac{M_D \boldsymbol{u}^H \boldsymbol{G}_B^H \boldsymbol{G}_B \boldsymbol{u}}{M_B \boldsymbol{u}^H \boldsymbol{G}_D^H \boldsymbol{G}_D \boldsymbol{u}}, \tag{15}$$

where the ^{H} superscript indicates the conjugate transpose operator. The acoustic contrast is a dimensionless quantity, which is usually expressed in decibels with its level defined as $10 \log_{10} C$.

The above definition allows for the formulation of a constrained optimization problem. The most useful formulation aims to minimize $\boldsymbol{p}_D^H \boldsymbol{p}_D$ under the constraint that $\boldsymbol{p}_B^H \boldsymbol{p}_B$ is held constant, which also provides the practically useful solution[34]. The resulting Lagrangian is

$$\mathfrak{L} = \boldsymbol{p}_D^H \boldsymbol{p}_D - \lambda_1 (\boldsymbol{p}_B^H \boldsymbol{p}_B - B), \tag{16}$$

where λ_1 is the real and positive Lagrange multiplier, and B is the fixed constraint value. The vector $\boldsymbol{u}$ that minimizes this Lagrangian also maximizes the acoustic contrast. This solution corresponds to the eigenvector corresponding to the largest eigenvalue in the relation[34]

$$\lambda_1 \boldsymbol{u} = \left[\boldsymbol{G}_D^H \boldsymbol{G}_D\right]^{-1} \left[\boldsymbol{G}_B^H \boldsymbol{G}_B\right] \boldsymbol{u}. \tag{17}$$

Using the values of this eigenvector to generate the driving signal for the array achieves the highest level of acoustic contrast in the radiated sound field that the system is capable of

producing. It should be noted that alternative control methods, such as pressure matching[35] or planarity control[36] may allow an improvement in the audio quality, but this comes at the expense of reduced contrast between the bright and dark zones and so will not be considered further here.

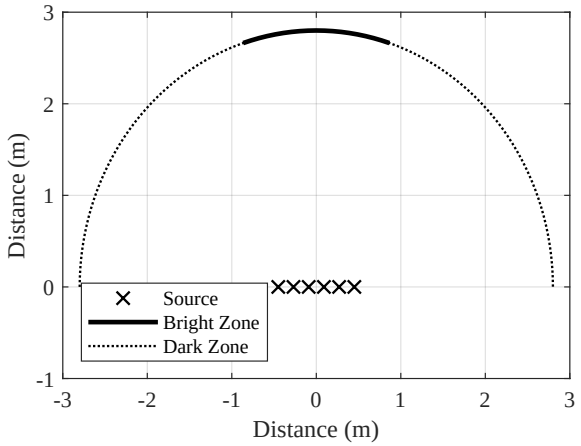

FIG. 3. Example distribution of bright and dark zones relative to an array of acoustical sources.

B. Array effort regularization

Another quantity that is useful for both the performance evaluation and optimization of an array is the normalized array effort. This is defined here as the sum of the modulus squared signals driving the array, divided by the modulus squared signal required from a single element at the centre of the array to produce the same mean square pressure in the bright zone, u_m. This has the form

$$AE = \frac{\boldsymbol{u}^H \boldsymbol{u}}{|u_m|^2}, \tag{18}$$

and is proportional to the electrical power required to drive the array, if one assumes that no significant electroacoustic interactions between the transducers occur[37]. As with the acoustic contrast, the array effort is a dimensionless quantity, again expressed in decibels and with a level defined as $10\log_{10} AE$.

When formulating the optimization problem defined by Eq. (16), it is generally of practical benefit in terms of the system robustness to introduce an additional constraint on the array effort and this has been investigated in[34]. In this case, the sum of the squared pressures in the dark zone, $\boldsymbol{p}_D^H\boldsymbol{p}_D$, is still minimized, but under the constraints that both $\boldsymbol{p}_B^H\boldsymbol{p}_B$ is equal to B and that $\boldsymbol{u}^H\boldsymbol{u}$ is equal to P, which represents a constraint on the total power of the signals driving the array. The corresponding Lagrangian has the form

$$\mathfrak{L} = \boldsymbol{p}_D^H\boldsymbol{p}_D + \lambda_1(\boldsymbol{p}_B^H\boldsymbol{p}_B - B) + \lambda_2(\boldsymbol{u}^H\boldsymbol{u} - P), \tag{19}$$

where λ_1 and λ_2 are the positive real values of the Lagrange multipliers. Seeking the minimum solution of this Lagrangian has been shown to lead to the relation

$$\lambda_1\boldsymbol{u} = -\left[\boldsymbol{G}_B^H\boldsymbol{G}_B\right]^{-1}\left[\boldsymbol{G}_D^H\boldsymbol{G}_D + \lambda_2\boldsymbol{I}\right]\boldsymbol{u}. \tag{20}$$

The optimal solution in this case can be obtained from the eigenvector corresponding to the largest eigenvalue of the inverse matrix, $\left[\boldsymbol{G}_D^H\boldsymbol{G}_D + \lambda_2\boldsymbol{I}\right]^{-1}\left[\boldsymbol{G}_B^H\boldsymbol{G}_B\right]$. In this case, the Lagrange multiplier, λ_2, not only limits the array effort, but also regularizes the matrix being inverted, which can improve the robustness of the system in practice[34].

IV. PARAMETRIC DESIGN STUDY

The mathematical model that has been formulated in Sec. II can be used to simulate the radiated sound field of the actuator array and vibrating panel system. This section will present a simulation based study into the effect certain design parameters, such as the panel dimensions and the actuator array distribution, have on the directivity performance of the system.

For a more effective comparison with the results of the physical measurements to be presented in the next section, the acoustic contrast control zones are defined by eleven pressure measurement points distributed evenly on a 2.8 m radius half-circle in the designated forward half-space, centred around the array, as shown in Fig. 3. The bright zone corresponds to a 36° arc, which is defined by three measurement points regardless of the array steering direction, with the remaining measurement points comprising the dark zone. All simulations to be presented in this, and in subsequent sections, consider 50 modes along the x-direction and 30 modes along the y-direction, giving a total of 1500 modes in the structural model of the panel. This number has been chosen so as to ensure an accurate approximation of the theoretically infinite summations in Eq. (6), and therefore an accurate representation of the structural response within the frequency range investigated in this study.

A. Panel size

The first part of the parametric study explores the effects of the panel size on the array directivity. Figure 4 shows the average value of acoustic contrast calculated for frequencies

between 100 Hz and 5 kHz, as a function of panel length in (a) and (b), and of panel width in (c). By varying the length of the panel one also affects the relative positions of the actuators from its edges. Results are expected to differ when the overall array length is kept fixed while the length of the panel is increased, and when the spacing between the actuators is also changed to ensure that they are evenly distributed along the length of the panel, thus increasing the overall array length. Although loudspeaker arrays can use a non-uniform spacing between their elements to increase the aliasing frequency, this is less important in the structural actuator array due to the effective interpolation between the sources. It turns out that it is more beneficial to evenly distribute the actuators so that they effectively couple into the maximum number of modes and thus allow greater control of the structural response. Figure 4 (a) shows the frequency averaged contrast versus panel length for these two actuator distributions for a forward directed bright zone. It is evident from these results that performance in both cases increases as the length of the panel is increased. For longer panel lengths it can also be seen that there is a small advantage to evenly distributing the actuators along the length of the panel, rather than keeping their positions fixed. In Fig. 4 (b), the frequency averaged acoustic contrast is shown for the case where the bright zone is steered to 54°. In this setting it is clear that an even distribution along the panel is capable of much higher levels of acoustic contrast.

Finally, Fig. 4 (c) shows the frequency averaged acoustic contrast as a function of the width of the panel, for the case when the actuators are evenly distributed along its length and the beam is steered in either the forward or 54° direction. From these results it can be seen that when considering the contrast performance in the horizontal plane, the width

of the panel does not have a significant influence on the performance, irrespective of the steering angle. If the directivity in the vertical plane was considered, then the width of the panel would, however, have an equivalent influence to the panel length in the horizontal plane and this may be important in different realisations.

B. Actuator array distribution

In the previous section it has been shown in brief that the distribution of the actuators on the panel has a significant impact on the achievable acoustic contrast, particularly when the bright zone is steered away from the forward direction. Therefore, it is important to also investigate the effects of changing the array distribution in isolation, without any other changes to the system parameters. The optimization of the actuator distribution on a flat panel loudspeaker has been previously investigated with the objective of matching the frequency response of a conventional loudspeaker[38]. However, in this instance, the aim is to ensure a high degree of directivity across a wide frequency range, rather than matching the performance of a traditional cone loudspeaker. Keeping the dimensions of the panel fixed at 1000 mm $\times$ 200 mm $\times$ 3 mm, the effect of different actuator array distributions has thus been investigated.

The average acoustic contrast between 100 Hz and 5 kHz as a function of the spacing between consecutive actuators, for different numbers of actuators, is shown in Fig. 5 (a). The bright zone is set to the forward direction for all cases. It is evident that by increasing the number of actuators, the overall performance improves. The difference in frequency averaged contrast is much greater when increasing the number of actuators from an even to

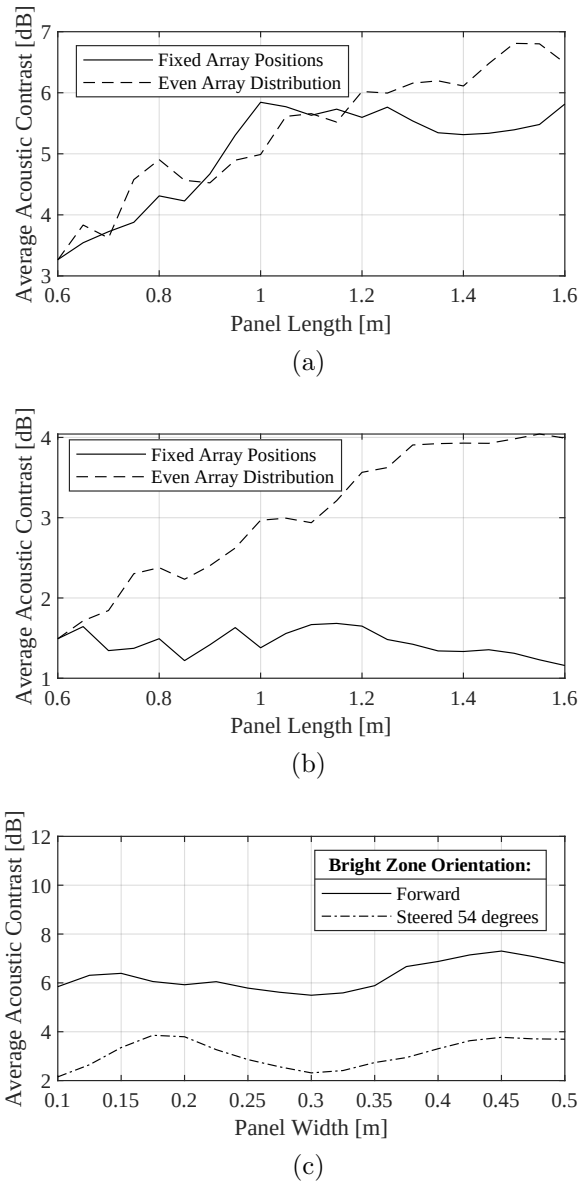

FIG. 4. Frequency averaged acoustic contrast between 100 Hz and 5 kHz for a simulated panel of varying size. Effects of different panel lengths for a bright zone in the forward direction are shown in (a), and steered by 54° in (b), with different lines corresponding to the distribution of the array actuators. In (c) the frequency averaged contrast is shown as a function of panel width for the forward and steered setting, for an even array distribution alonth the length of the panel.

an odd number than when increasing it from odd to even. This is due to the presence of an actuator at the centre of the panel being beneficial to the generation of a forward directed sound field. Thus, when increasing the number of actuators from seven to eight, for example, the even distribution of the array on the panel means that there is no longer an actuator at the center point of the panel, which limits the achieved improvement in directivity. The spacing between actuators seems to only have a limited effect, with a slight downward trend in frequency averaged contrast as the distance is increased.

In Fig. 5 (b) the acoustic contrast frequency response is shown for arrays of six actuators using different spacings. In conjunction with the results in Fig. 5 (a), it can be seen that although the average contrast over the presented frequency range shows little change with different array distributions, it is different for isolated frequencies. At frequencies above around 400 Hz, the location of peaks and dips in the contrast is greatly dependent on the chosen actuator spacing. This effect needs to be taken into account when designing a system intended for specific frequency ranges, as it should be appropriately tuned to maximize the performance across the desired frequency region.

In summary, the parametric study has shown that for the presented configurations, the acoustic contrast performance of the structural actuator based array is dependent on the length of the panel, the number of actuators and their distribution on the panel. Longer panels, as well as a greater number of actuators in the array generally ensure a higher overall contrast over the investigated frequency range. The frequencies at which maximum contrast is achieved is dependent on the spacing between actuators. For steered settings, an even

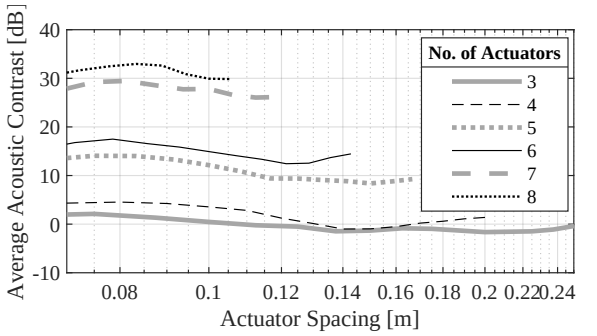

(a)

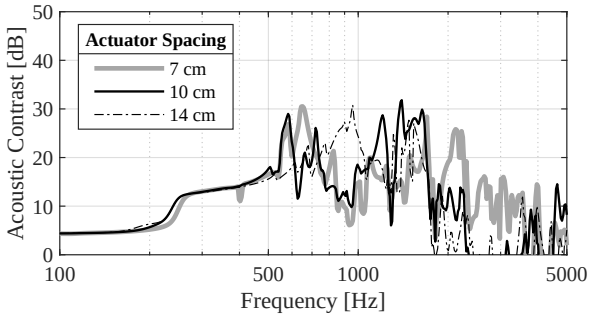

(b)

FIG. 5. Simulated effect of different array distributions on a 1 m long rectangular panel. In (a) the frequency averaged acoustic contrast for different array sizes is depicted. (b) shows the acoustic contrast frequency response for six actuators with different inter-element spacings.

distribution of the array elements along the panel is necessary to achieve significant contrast, although overall performance is still lower than for the forward focused array.

V. EXPERIMENTAL IMPLEMENTATION

Based on the understanding gained from the simulation-based study presented in Sec. IV, a prototype system has been assembled, and shown in Fig. 6. The prototype consists of an array of six round audio actuators, as shown in Fig. 6 (a), with an overall weight of 360 g and a nominal frequency range from 200 Hz to 20 kHz. This array is attached to

a 1000 mm× 200 mm× 3 mm 6082 aluminium alloy panel and is distributed evenly along the length of the panel, with a 14.3 cm spacing between consecutive actuators. The panel itself is set upon a wooden mounting, which creates an enclosure of dimensions 1000 mm× 200 mm× 180 mm. Constraints on the frequency range within which the system can be reliably evaluated and compared with the mathematical model are primarily imposed by the additional mass loading on the panel due to the weight of the actuators at lower frequencies, and by the number of modes included in the model at higher frequencies. The prototype is used to both validate the results presented in the previous section and to assess the potential performance of the proposed directional structural-actuator array system in practice.

A. Measurement process

The prototype system was tested in the large anechoic chamber at the Institute of Sound and Vibration Research. The array was placed at the centre of the anechoic chamber at a height of 1 m, as shown in Fig. 6 (c). Also shown in this photograph is the microphone array used for the measurements. Eleven microphones cover the forward half-plane, in a half-circle arrangement at a height of 1.1 m, which coincides with the exact height of the actuator array. and at radial distance from the centre of the array of 2.8 m, which is limited by the dimensions of the anechoic chamber. The actuators were driven by 15 W class D audio amplifiers, and were controlled via a compact data acquisition system. All measurements and simulations consider only the forward half-space, and wedges of fibreglass were inserted in the rear enclosure of the prototype to reduce unwanted sound radiation from the rear of the panel, and minimize the potential discrepancies caused by this factor. However, the

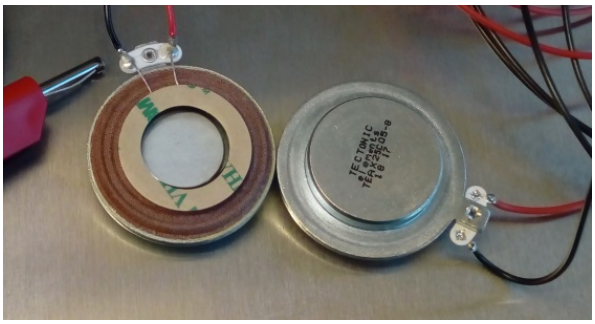

(a)

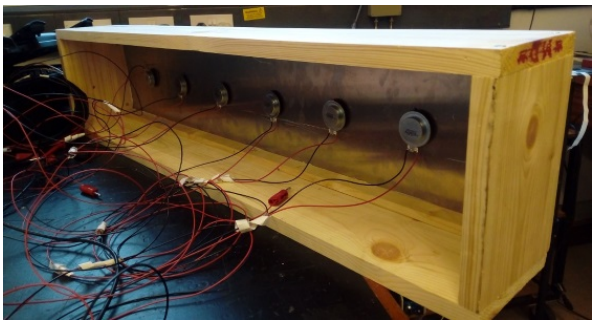

(b)

(c)

FIG. 6. (color online) Example pair of audio actuators used in the prototype system (a). The actuator array as attached to the metal panel and its wooden mounting is also shown in (b). The set-up of the measurements in the anechoic chamber is shown in (c).

fact that the analytical model assumes the panel is positioned in an infinite baffle, which is distinct from the experimental conditions, is still expected to have an effect on the accuracy of the predictions made.

Initially, each actuator was driven separately using a swept sine wave signal of 60 s duration, covering frequencies from 100 Hz to 5 kHz. These measurements were utilized to estimate the individual frequency response from each actuator to each of the measurement microphones. The responses from the six actuators to the eleven microphones were then used to construct the matrix of complex transfer responses, $\boldsymbol{G}(\omega)$. For the measurements

presented in this paper, only the forward half-space is to be considered when estimating the acoustic contrast, to ensure consistency with the mathematical model based simulations, as the assumption of an infinite baffle in the formulation of the model is expected to have different effects compared to the frame upon which the prototype is mounted. From $\boldsymbol{G}(\omega)$ it is possible to define the two transfer matrices corresponding to points in the bright and dark zones, $\boldsymbol{G}_B(\omega)$ and $\boldsymbol{G}_D(\omega)$. The control zones used in the experimental set-up have the same definitions as the control zones used in Sec. IV. The bright zone is defined by three microphones, which cover a 36° angle. Figure 7 shows the control zones used, with the bright and dark zones chosen to maximize directivity in the forward direction.

From the two frequency response matrices defined above it is possible to calculate the optimum off-line acoustic contrast using Eqs. (15) and (20). A set of six FIR filters, one corresponding to each actuator, can then be designed to match the frequency response of the optimal frequency domain driving signals, $\boldsymbol{u}$, which are given by Eq. (20). On-line directivity control is thus achieved by applying these filters to the signal driving the array. In the following section, the performance of the array is investigated through a series of measurements, which are compared to the corresponding theoretical results obtained through simulations.

B. Experimental results

A first step in the experimental validation process is to compare the frequency response of the system as simulated and as measured. Figure 8 shows the structural response of the system when driven by a single actuator, measured using an accelerometer located at a

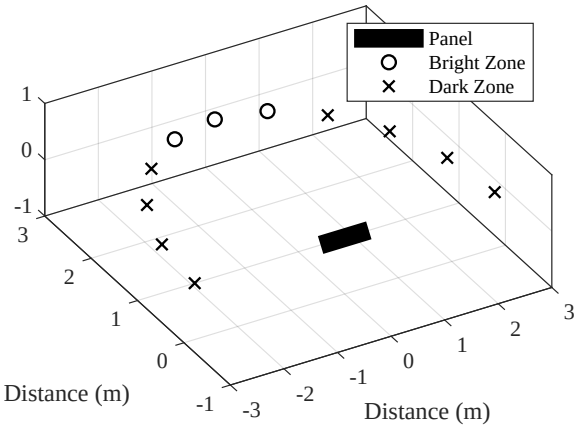

FIG. 7. The control zone used for the measurements in the anechoic chamber. Open circles represent microphones comprising the bright zone, and black dots represent the dark zone microphones. The dark line denotes the space occupied by the prototype system.

point with coordinates (0.24 m, 0.07 m) on the panel; the corresponding simulation result, as calculated using Eq. (6), is also shown. This comparison between the simulated and measured results shows that the model matches the behaviour of the physical system well for frequencies ranging from 400 Hz to roughly 3 kHz. At lower frequencies, differences between the simulated and measured responses are more noticeable. This is because the analytical model does not consider the mass of the actuators. In reality, this additional mass loading on the panel has an effect in its response at these frequencies. Potential causes for other discrepancies between the measurement and simulation results across the entire frequency range are the representation of the actuators by distributions of point forces, the infinite baffle assumption and the simply supported boundary conditions in the model.

The on-axis sound pressure level frequency response, measured at a distance of 2.8 m from the centre of the panel is evaluated and the measurement is compared to the simulation, cal-

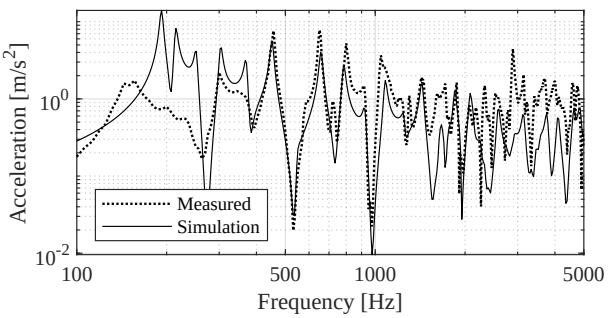

FIG. 8. Structural response of the system, as measured at a point of coordinates (0.24 m, 0.07 m) on the panel. Comparison between simulation and measured data.

culated from Eq. (13), in Fig. 9. Comparison of the results shows that for frequencies above 400 Hz the response of the model effectively follows the trends of the physical prototype. Once again, discrepancies are most likely due to neglecting the mass of the actuators, and other approximations such as the simply supported boundary conditions and the assumption of an infinite baffle in the model.

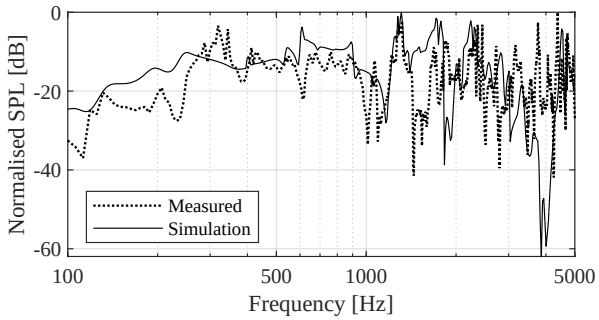

FIG. 9. On-axis sound pressure level frequency response at a distance of 2.8 m. Comparison between simulation and measured data.

Directivity control is achieved using the prototype system by driving the actuators with an output signal filtered through their respective FIR filters, as described in Section V A.

The sound pressure level measured by the microphone array is used to calculate the acoustic contrast using Eq. (15). In Figure 10, the average measured sound pressure level calculated between 300 Hz and 3 kHz, is shown for different steering settings: aimed forward, and at angles of 36°, 54° and 72°. In all cases the bright zone has a coverage width of 36°. The frequency limits in this instance were chosen to lie within the effective operating bandwidth of the prototype. It is evident from these plots that the system is capable of controlled directional radiation. In order to obtain a more in-depth view of its performance, however, it is necessary to examine the directional characteristic as a function of frequency.

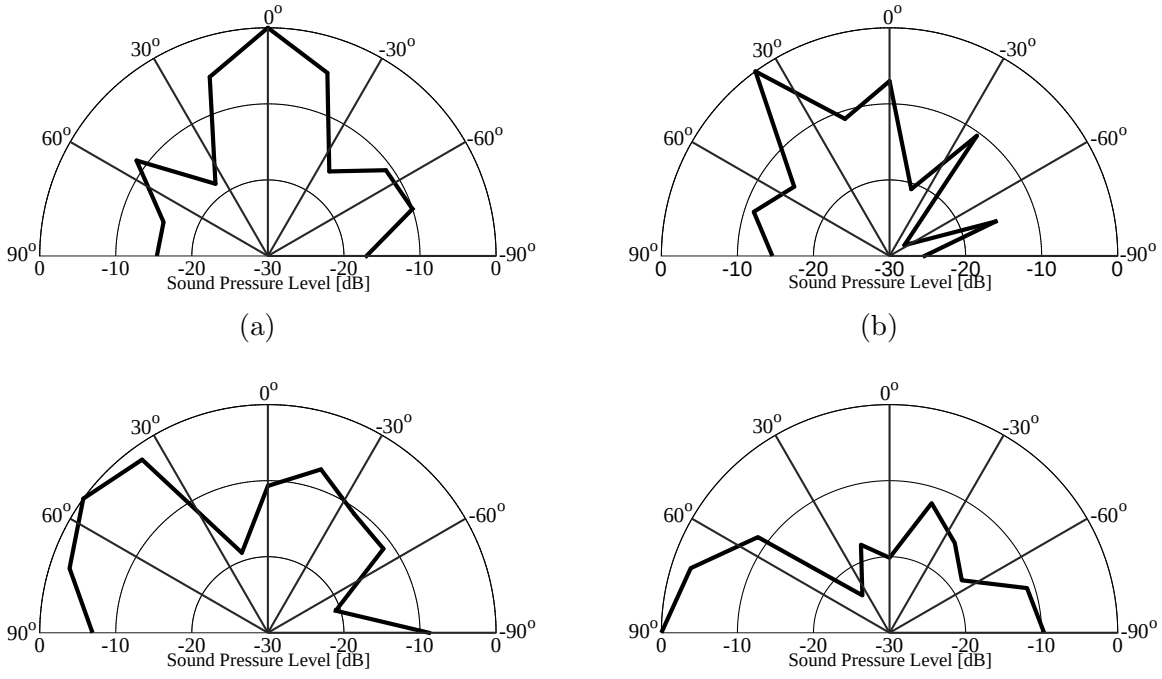

FIG. 10. Average sound pressure level between 300 Hz and 3 kHz, as measured with the prototype in an anechoic chamber using a 36° wide bright zone centred in the forward direction (a), steered by 36° (b), steered by 54° (c), and steered by 72° (d).

Figure 11 shows the acoustic contrast over frequency, calculated according to Eq. (15). For the simulation and measurement results of the prototype system, for different directivity settings. The regularization factor, λ_2, used in the measurements, is chosen to ensure a relatively smooth response, as elaborated in Sec. V A. The value chosen for λ_2 in the simulations is set so that the simulated system requires equal array effort to the measured system. This is done to ensure a fair comparison. In all cases, the model is effective at predicting the trends exhibited by the physical system over frequency. The accuracy of the predictions appears to diminish as the steering angle increases, particularly at the lower end of the investigated frequency range.

The system achieves the highest average acoustic contrast over the investigated frequency range, as well as the highest value for contrast at an isolated frequency, for the forward setting. As the steering angle is shifted to 36° and then to 54°, the average contrast decreases, which is due to the effective decrease in the aperture size. It is worth noting however, that a limited increase in contrast is visible for frequencies above 2 kHz. For the 72° steered setting, along with the increase at higher frequencies, there is also a significant improvement in performance at lower frequencies around the 500 Hz mark. As the steering angle approaches 90°, the arrangement of actuators begins to resemble that of sound sources in an end-fire instead of broadside configuration, which is also capable of high directivity[39,40]. However, due to the finite size of the plate, standing waves occur and the resulting modal behaviour imposes a limitation on the end-fire capabilities of the system, which would otherwise require an infinite surface. From these results, it can be concluded that the structural vibration and

418 sound radiation of the plate can be controlled in a similar way to an array of individual
419 sound sources.

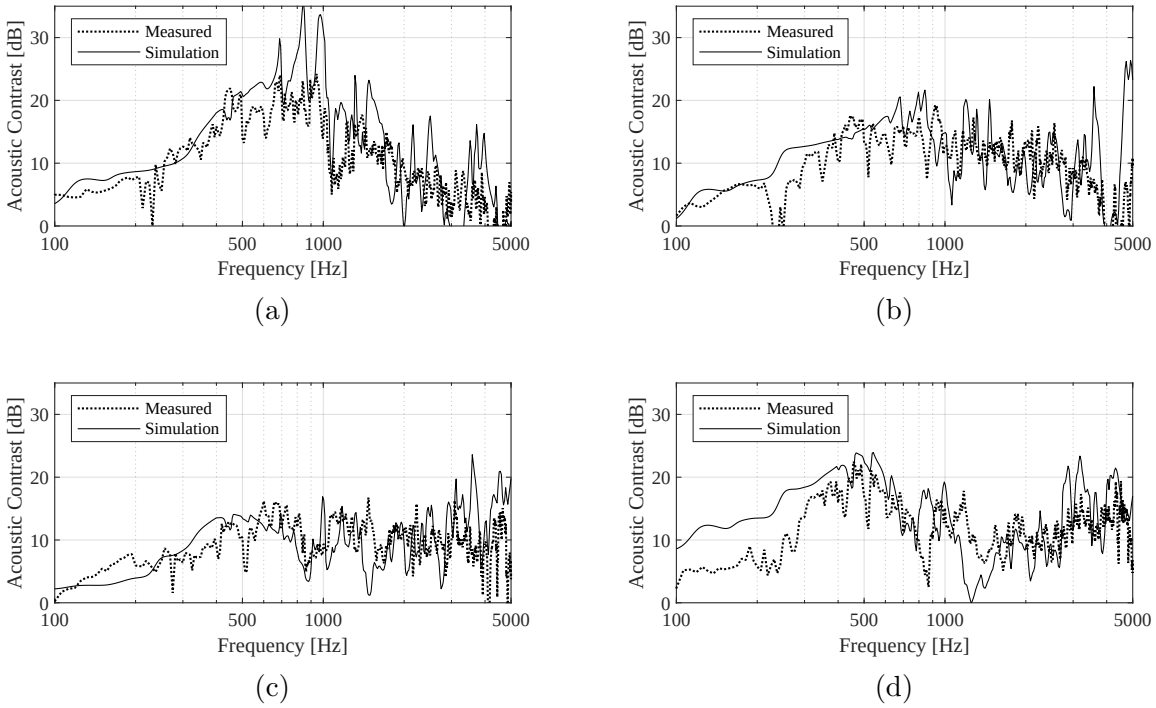

FIG. 11. Comparison of the acoustic contrast response over frequency between simulations and measurements for a 36° wide bright zone centred in the forward direction (a), steered by 36° (b), steered by 54° (c), and steered by 72° (d).

420 VI. CONCLUSIONS

421 This paper proposed and investigated a means of generating a directional sound field
422 by controlling the structural vibration of a panel. The presented system consists of a flat
423 rectangular panel with simply supported edges, and an array of inertial actuators distributed
424 over its surface, which force the structural response to achieve a controlled radiation pattern.

An analytical mathematical model was formulated by considering the vibration of a thin rectangular panel excited by multiple point forces, and the resulting radiated sound pressure in the far field. Directivity control was achieved through the acoustic contrast maximization process, which produces the necessary amplitude and phase with which to drive each actuator.

Using this model, a simulation based parametric study was carried out to determine how the dimensions of the panel and the distribution of actuators on its surface affect its directivity performance. Results show that a longer panel and a greater number of actuators in the array achieve a higher acoustic contrast on average over an operating bandwidth of 100 Hz to 5 kHz, while an even distribution of actuators ensures better performance when the beam is steered at angles away from the normal, or forward direction.

A prototype system comprising of an aluminium panel mounted within a wooden enclosure, with an array of six inertial actuators was assembled and tested in an anechoic environment. The directivity performance of the system was shown to be frequency dependent, and most effective when steered in the forward direction. Comparison between the measured results and the simulations indicated that the model provides a useful indication of the expected behaviour of the system within the 400 Hz to 3 kHz range. Inaccuracies between the model and the measurements did occur, however, particularly at lower frequencies. These inaccuracies were due to physical characteristics not considered in the model such as the size and mass of the inertial actuators, as well as the simply supported boundary conditions used in the model.

Overall, the system has been shown to be capable of radiating a directional sound field. The analytical model presented can be used to determine the optimal design parameters for the system to maximize its performance within a desired frequency range, whilst considering practical limitations on panel size and number of actuators.

ACKNOWLEDGMENTS

The authors gratefully acknowledge the European Commission for its support of the Marie Sklodowska Curie program through the ETN PBNv2 project (GA 721615).

REFERENCES

[1]D. G. Meyer "Digital control of loudspeaker array directivity," J. Audio Eng. Soc. **274**, 605–619 (2004).

[2]I. Tashev, J. Droppo, M. Seltzer, A. A. Acero "Robust design of wideband loudspeaker arrays," IEEE International Conference on Acoustics, Speech and Signal Processing 381-384 (2008).

[3]I. Tashev "Loudspeaker array design," J. Acoust. Soc. Am. **127**, 3100 (2013).

[4]M. A. Poletti, F. M. Fazi, P. A. Nelson "Sound-field reproduction systems using fixed-directivity loudspeakers," J. Acoust. Soc. Am. **134**, 3590-3601 (2010).

[5]M. A. Poletti, F. M. Fazi, P. A. Nelson "Sound reproduction systems using variable-directivity loudspeakers," J. Acoust. Soc. Am. **129**, 1429-1438 (2011).

[6]C. Shi, W. Gan "Grating lobe elimination in steerable parametric loudspeaker," IEEE Transactions on Ultrasonics, Ferroelectrics, and Frequency Control **58**, 437-450 (2011).

[7]J. Cheer, S. J. Elliott, M. F. Simón Gólvez "Design and Implementation of a Car Cabin Personal Audio System," J. Audio Eng. Soc. **61**, 412-424 (2013).

[8]M. F. Simón Gálvez, S. J. Elliott, J. Cheer "Personal audio loudspeaker array as a complementary TV sound system for the hard of hearing," IEICE Transactions on Fundamentals of Electronics, Communications and Computer Sciences **97**, 1824-1831 (2014).

[9]R. Van der Rots, A. Berkhoff "Directional loudspeaker arrays for acoustic warning systems with minimised noise pollution," Applied Acoustics **89**, 345-354 (2015).

[10]F. J. Pompei "Directional acoustic alerting system," US Patent 7,106,180 (2006).

[11]J. A. S. Angus "Distributed mode loudspeaker polar patterns," Audio Engineering Society Convention 107 (1999).

[12]V. P. Gontcharov, N. P. R. Hill "Diffusivity properties of distributed mode loudspeakers," Audio Engineering Society Convention 108 (2000).

[13]P. Newell, K. R. Holland *Loudspeakers: For music recording and reproduction,* Routledge (2006).

[14]D. A. Anderson, M. F. Bocko "Modal Crossover Networks for Flat-Panel Loudspeakers," J. Audio Eng. Soc. **64**, 229-240 (2016).

[15]R. Rabenstein, S. Spors, Sascha "Spatial Aliasing Artifacts Produced by Linear and Circular Loudspeaker Arrays used for Wave Field Synthesis," Audio Engineering Society Convention **120**, (2006).

[16]N. Kournoutos, J. Cheer, S. J. Elliott "The design of a low-cost directional warning sound system for electric vehicles," Proceedings of the 43rd International Conference on Noise and Vibration Engineering (ISMA) (2018).

[17]R. J. Hannon "Vibration and sound radiation of a plate," J. Acoust. Soc. Am. **58**, 543 (1975).

[18]C. R. Fuller, C. H. Hansen, S. D. Snyder "Experiments on active control of sound radiation from a panel using a piezoceramic actuator," Journal of Sound and Vibration **150**, 179-190 (1991).

[19]C. Paulitsch, P. Gardonio, S. J. and Elliott "Active vibration control using an inertial actuator with internal damping," J. Acoust. Soc. Am. **119**, 2131-2140 (2006).

[20]C. Deffayet, P. A. Nelson "Active control of low frequency harmonic sound radiated by a finite panel," J. Acoust. Soc. Am. **84**, 2192-2199 (1988).

[21]J. Pan, S. D. Snyder, C. H. Hansen, C. R. Fuller "Active control of far-field sound radiated by a rectangular panel –A general analysis," J. Acoust. Soc. Am. **91**, 2056-2066 (1992).

[22]C. R. Fuller, C.H. Hansen, S.D. Snyder "Active control of sound radiation from a vibrating rectangular panel by sound sources and vibration inputs: An experimental comparison," Journal of Sound and Vibration **145**, 195-215 (1991).

[23]D. A. Anderson, M. C. Heilemann, M. F. Bocko "Measures of vibrational localization on point-driven flat-panel loudspeakers," Proceedings of Meetings on Acoustics **26**, 65-73 (2016).

[24]Q. Li, D. J. Thompson "Directivity of sound radiated from baffled rectangular plates and plate strips," Applied Acoustics **155**, 309-324 (2019).

[25]L. Cremer, M. Heckl *Structure-borne sound: structural vibrations and sound radiation at audio frequencies,* Springer (1988).

[26]L. Meirovitch *Analytical methods in vibrations,* McMillan (1967).

[27]G. B. Warburton "The Vibration of Rectangular Plates," Proceedings of the Institution of Mechanical Engineers **168**, 371-384 (1954).

[28]C. R. Fuller, S. J. Elliott, P. Nelson *Active control of vibration,* Academic Press (1996).

[29]D. A. Anderson, and M. C. Heilemann, and M. F. Bocko "Flat-Panel Loudspeaker Simulation Model with Electromagnetic Inertial Exciters and Enclosures," J. Audio Eng. Soc **65**, 722-732 (2017).

[30]C. E. Wallace " Radiation Resistance of a Rectangular Panel ," J. Acoust. Soc. Am. **51**, 946-952 (1972).

[31]S.J. Elliott, J. Cheer, H. Murfet, K. R. Holland "Minimally radiating sources for personal audio," J. Acoust. Soc. Am. **128**, 1721-1728 (2010).

[32]J-Y. Park, J-H. Chang, Y-H. Kim "Generation of Independent Bright Zones for a Two-Channel Private Audio System," J. Audio Eng. Soc. **58**, 382-393 (2010).

[33]J-W. Choi, Y-H. Kim "Generation of an acoustically bright zone with an illuminated region using multiple sources," J. Acoust. Soc. Am. **111**, 1695-1700 (2002).

[34]S. J. Elliott, J. Cheer, J-W. Choi, Y-H. Kim "Robustness and Regularization of Personal Audio Systems," IEEE Transactions on Audio, Speech, and Language Processing **20**,

2123-2133 (2012).

[35]F. Olivieri, F. M. Fazi, and M. Shin, P. Nelson "Pressure-Matching Beamforming Method for Loudspeaker Arrays with Frequency Dependent Selection of Control Points," Audio Engineering Society Convention 138 (2015).

[36]P. Coleman, P. J. B. Jackson, M. Olik, M. Mller, M. Olsen, J. Abildgaard Pedersen "Acoustic contrast, planarity and robustness of sound zone methods using a circular loudspeaker array," J. Acoust. Soc. Am. **135**, 1929-1940 (2014).

[37]M. F. Simón Gálvez, S. J. Elliott, J. Cheer "A superdirective array of phase shift sources," J. Acoust. Soc. Am. **132**, 746-756 (2012).

[38]D. A. Anderson, M. C. Heilemann, M. F. Bocko "Optimized Driver Placement for Array-Driven Flat-Panel Loudspeakers," Archives of Acoustics **42**, 93-104 (2017).

[39]M. M. Boone, W-H. Cho, J-G. Ih "Design of a Highly Directional Endfire Loudspeaker Array," J. Audio Eng. Soc. **57**, 309-325 (2009).

[40]K. R. Holland, F. J. Fahy "A Low-Cost End-Fire Acoustic Radiator," J. Audio Eng. Soc. **39**, 540-550 (1991).